NUKLEONIKA 2015;60(2):355–360
doi: 10.1515/nuka-2015-0036

ORIGINAL PAPER

DE GRUYTER
OPEN

Enhanced resonant second harmonic generation in plasma based on density transition

**Niti Kant,
Vishal Thakur**

Abstract. Resonant second harmonic generation of a relativistic self-focusing laser in plasma with density ramp profile has been investigated. A high intense Gaussian laser beam generates resonant second harmonic beam in plasma with density ramp profile. The second harmonic undergoes periodic focusing in the plasma channel created by the fundamental wave. The normalized second harmonic amplitude varies periodically with distance and attains maximum value in the focal region. Enhancement in the second harmonic amplitude on account of relativistic self-focusing of laser based on plasma density transition is seen. Plasma density ramp plays an important role to make self-focusing stronger which leads to enhance the second harmonic generation in plasma.

Key words: second harmonic generation • laser • plasma density ramp • self-focusing

N. Kant✉, V. Thakur
Department of Physics,
Lovely Professional University,
G. T. Road, Phagwara – 144411, Punjab, India,
E-mail: nitikant@yahoo.com

Received: 25 September 2014
Accepted: 22 January 2015

Introduction

The interaction of high power laser beams with plasmas and semiconductors, plays a very important role in the study of various nonlinear phenomena, e.g. harmonic generation, frequency up-conversion, signal processing, etc. [1–5]. Harmonic generation during high power laser interaction with plasmas is observed under different conditions [6, 7]. The interaction of ultra-intense laser beam with plasma also produces second harmonic generation by inducing transverse plasma currents which is highly nonlinear and relativistic, resulting in the generation of second harmonic current density which drive the second harmonic generation.

Second harmonic generation during laser plasma interaction has become more prominent. Although, the efficiency of harmonic generation observed during laser plasma interaction is quite low. A number of techniques have been employed to enhance the efficiency of harmonic generation, out of these, effect of self-focusing of fundamental laser beam has shown great importance on harmonic generation [8, 9]. Relativistic self-focusing of the laser beam has been studied in detail both theoretically as well as experimentally [10]. As the process of harmonic generation is non-resonant, so to make the process resonant various schemes are proposed by various researchers [3, 7, 11, 12]. It has been found that in order to provide additional momentum to the harmonic photon to make the process resonant which leads to enhance the efficiency of harmonic generation, the effect of plasma with density ripple and Wiggler magnetic field can be introduced.

In order to obtain efficient harmonic generation, phase matching condition must be satisfied. Osman *et al.* [13] have studied resonant harmonic generation of intense laser in plasma. Hafizi *et al.* [14] have derived an envelope equation for the laser spot size to describe the axial evolution of the spot size as a function of the ratio of laser power P to the critical power P_c for relativistic focusing. Hora and Ghatak [15] have derived and evaluated by including unrestricted electric fields, a second harmonic resonance for perpendicular incidence at four times the critical density, from hydrodynamics. Also second harmonic emission in the forward direction from an under dense plasma has been observed experimentally by Baton *et al.* [16]. The simultaneous observation of time-resolved and 2D time-integrated images of second harmonic generation has been reported by them. These diagnostics have a good spatial and temporal resolution, allowing the detection of second harmonic emission in small and well-defined regions. Schifano *et al.* [17] have observed the second harmonic generation from preformed plasma as a valuable diagnostic for filamentation under various interaction conditions. Ganeev *et al.* [18] have presented experimental study on harmonic generation from solid surface irradiated by short laser pulses. The relative harmonic yield for the P and S polarization of the pump wave and their scaling with laser intensity are discussed. High harmonic generation in relativistic laser–plasma interaction has also been studied by Banerjee *et al.* [19]. They showed that relativistic Thomson scattering produces a significant amount of harmonic radiation. A nonlinear theory for harmonic generation of a high power laser in under dense plasma has been proposed by Lin *et al.* [20]. In their theory, harmonic sideband generation is related to the transition of system equilibrium states. Their numerical results revealed that laser power and plasma density parameters are crucial to harmonic generation.

In this paper we present a model to enhance the efficiency of second harmonic generation. We propose a scheme to introduce a density ramp profile in plasma which plays an important role in self-focusing which leads to enhance the second harmonic generation in plasma. We consider the plasma density as a function of propagation distance. The dependence of relativistic self-focusing and plasma density on second harmonic generation has been studied. As the plasma density ramp is introduced, the fundamental laser beam propagates up to long distance without divergence [8, 21–24]. Therefore, relativistic self-focusing of fundamental laser beam becomes stronger which greatly enhances the intensity and hence the efficiency of the second harmonic generation.

In the next section, we derive the equation of beam width parameter of the fundamental laser beam, and the equation describing the variation of normalized amplitude of the second harmonic wave $A_{20}^{"}$ with normalized propagation distance ξ. The numerical results are discussed in section 'Relativistic self-focusing', and the conclusions are presented in the last section.

Theoretical considerations

Consider the propagation of Gaussian short pulse laser beam in a preformed plasma channel with an upward plasma density ramp along z-direction in the presence of a Wiggler magnetic field $\vec{B}_W$. The field of the laser beam can be written as

$$\vec{E}_1 = \hat{x}A_1(z,t)\exp[-i(\omega_1 t - k_1 z)] \tag{1}$$

$$A_1^2 = \frac{A_{10}^2}{f_1^2(z)}\exp\left[\frac{-r^2}{r_0^2 f_1^2}\right] \tag{1a}$$

$$\vec{B}_1 = \frac{c\vec{k}_1 \times \vec{E}_1}{\omega_1} \tag{1b}$$

$$\vec{B}_W = \hat{y}B_0\exp(ik_0 z) \tag{1c}$$

where A_1 is the amplitude of the fundamental laser pulse inside plasma, A_{10} is the constant amplitude of the fundamental laser pulse, r_0 is the spot size of the fundamental laser pulse at $z = 0$, f_1 is the beam width parameter of the fundamental laser pulse, ω_1 and k_1 are the frequency and wave number of fundamental laser beam and k_0 is the Wiggler wave number. The pump wave and the second harmonic wave obey the linear dispersion relation, $k^2 \approx (\omega^2/c^2)(1 - \omega_p^2/\omega^2)$. The wave vector $\vec{k}$ increases more than linearly with frequency ω, hence $k_2 > 2k_1$. The difference of momentum can be provided to the second harmonic photon by the Wiggler magnetic field when $\vec{k}_2 = 2\vec{k}_1 + \vec{k}_0$; the value of $\vec{k}_0$ required for the phase matching can be obtained as $k_0 = (2\omega_1/c)[(1 - \omega_p^2/4\omega_1^2)^{1/2} - (1 - \omega_p^2/\omega_1^2)]$, where $\omega_p = (4\pi(\xi)e^2/m)^{1/2}$ is the plasma frequency which is a function of propagation distance, $m = m_0\gamma$, where $\gamma = \sqrt{1 - v^2/c^2}$ and the plasma density profile [8] is taken as $n(\xi) = n_0 \tan(\xi/d)$, where $\xi = z/R_d$; $R_d = kr_0^2$; is the diffraction length, c is the velocity of light in vacuum, n_0 is the electron density, and e and m_0 are the charge and rest mass of the electron, respectively.

Let us consider the dielectric constant of the plasma which can be expressed as,

$$\varepsilon = \varepsilon_0 + \phi(EE^*) \tag{2}$$

Therefore, the plasma frequency can be written as,

$$\omega_p^2 = \left(\frac{4\pi n_0 e^2}{m_0\gamma}\right)\tan\left(\frac{\xi}{d}\right) = \left(\frac{\omega_{p0}^2}{\gamma}\right)\tan\left(\frac{\xi}{d}\right) \tag{3}$$

where $\gamma = \sqrt{1 + e^2 EE^*/c^2 m_0^2\omega_0^2}$. Now, in case of collisionless plasma, the nonlinearity in the dielectric constant is due to relativistic mass increase and ponderomotive force, and the nonlinear part of dielectric constant is given by

$$(4)\quad \phi\left(EE^*\right)=\frac{\omega_{p0}^2}{\omega_1^2\gamma}\tan\left(\frac{\xi}{d}\right)\left[1-\exp\left(\frac{3m_0}{4M}\alpha_1 EE^*\right)\right].$$

Relativistic self-focusing

Wave equation for fundamental wave can be deduced by using Maxwell's equations

$$(5)\quad \nabla^2\vec{E}-\frac{\varepsilon}{c^2}\frac{\partial^2\vec{E}}{\partial t^2}=\frac{\omega_P^2}{c^2}\vec{E}$$

The solution of this equation can be assumed as,

$$(6)\quad \vec{E}=A\left(x,y,z\right)\exp[i\left(\omega_1 t-k_1 z\right)]$$

where $k_1 = \sqrt{\omega_1^2 - \omega_{p0}^2 \tan(\xi/d)/\gamma}$ and $A(x,y,z)$ is the complex amplitude of the electric field.

We can express $A(x,y,z)$ as,
$A(x,y,z) = A_{0p}(x,y,z)\exp[-ik_1 s(x,y,z)]$, or

$$(7)\quad A\left(x,y,z\right)=A_{0p}\left(x,y,z\right)\cdot\exp\left[-i\frac{S\sqrt{\omega_1{}^2-\dfrac{\omega_{p0}^2\tan\left(\dfrac{z}{dR_d}\right)}{\gamma}}}{c}\right]$$

where A_{0p} and S and are real functions of x, y and z. Therefore, Eq. (5) can be written as,

$$(8)\quad \left(\frac{\partial^2}{\partial z^2}+\frac{\partial^2}{\partial r^2}+\frac{1}{r}\frac{\partial}{\partial r}\right)\vec{E}+\frac{1}{c^2}\left[\epsilon_0+\phi(EE^*)\right]\omega_1^2\vec{E}=\frac{1}{c^2}\left(\frac{4\pi n(\xi)e^2}{m_0\gamma}\right)\vec{E}$$

where $\epsilon = 1 - \omega_p^2/\omega_1^2$ and $\phi = \omega_p^2/\omega_1^2\ |1 - 1/(1 + a^2/2)^{1/2}|$, where $a = e^2|A|^2/m_0^2\omega_1^2c^2$.

Using Eqs. (6), (7) and (8), and separating the real and imaginary parts of the resulting equation. Then, to find a solution of these equations describing a Gaussian beam and satisfying the appropriate initial conditions we expand S as follows:

$$(9)\quad S=\beta(z)\frac{r^2}{2}+\phi(z)$$

where β represents the inverse of the radius of curvature of the wave front.

For an initially Gaussian beam,

$$(10)\quad A_0^2=\frac{A_{10}^2}{f^2(z)}e^{-r^2/r_0^2f^2}$$

where f represents the beam width parameter of the fundamental laser beam.

We obtain the equation of beam width parameter of the fundamental laser beam,

$$(11)\quad \frac{d^2f_1}{d\xi^2}=\frac{\dfrac{\omega_{p0}}{\sqrt{\gamma}\omega_1}\sqrt{1-\dfrac{\omega_{p0}^2}{\gamma\omega_1^2}}}{\left(1-\dfrac{\omega_{p0}^2}{\gamma\omega_1^2}\tan\left(\dfrac{\xi}{d}\right)\right)-\dfrac{\xi}{2d}\dfrac{\omega_{p0}^2}{\gamma\omega_1^2}\sec^2\left(\dfrac{\xi}{d}\right)}\cdot\left[\frac{2k_1'\omega_1\sqrt{\gamma}}{\omega_{p0}f_1^3}-\frac{k_1'A_{10}^2R_d^2}{\epsilon_0\, r_0^2}\frac{\epsilon_2\epsilon_S}{\epsilon_0}\frac{\omega_1\sqrt{\gamma}}{\omega_{p0}}\cdot\exp\left\{-\frac{\epsilon_2}{2\,\epsilon_0}\frac{A_{10}^2}{f_1^2}\right\}\right]$$

where $k_1' = k_1c/\omega_1$ and $\varepsilon_0 = 1 - (\omega_{p0}^2/\gamma\omega_1^2)\tan(\xi/d)$.

Equation (11) describes the variation of the beam width parameter f_1 with the normalized distance of propagation ξ. The first term on the right-hand side corresponds to the diffraction divergence of the beam and the second term corresponds to the convergence resulting from the nonlinearity. Following Nitikant and Sharma [10], the wave equation for second harmonic generation under relativistic effect can be written as,

$$(12)\quad \nabla^2\vec{E}_2-\left[\frac{4\omega_1^2-5\omega_p^2}{c^2}+\frac{4\omega_1^2}{c^2}\phi(E_1E_1^*)\right]\vec{E}_2=-\frac{8\pi\, i\omega_1}{c^2}\vec{J}_2^{NL}$$

where $\vec{J}_2^{NL} = [n_0e^4B_WE_1^2/4ic\omega_1^2m_0^3\gamma(\omega_1 + iv)](3k_1/4\omega_1+(k_1 + k_0)/(\omega_1 + iv))\hat{x}$.

The complementary solution of Eq. (12) is given by,

$$(13)\quad E_{21}=A_2\exp\{-ik_2S_2\}\exp[-i(2\omega_1t-k_2z)]$$

where S_2 is a function of r and z. Using Eqs. (12) and (13), and equating real and imaginary parts,

$$(14)\quad 2\frac{\partial S_2}{\partial z}-\left(\frac{\partial S_2}{\partial z}\right)^2-\left(\frac{\partial S_2}{\partial r}\right)^2+\frac{1}{k_2{}^2A_2}\left(\frac{\partial^2A_2}{\partial r^2}+\frac{1}{r}\frac{\partial A_2}{\partial r}\right)-1+\frac{4\omega_1{}^2-5\dfrac{\omega_{p_0}^2}{\gamma\omega_1^2}\tan\left(\dfrac{\xi}{d}\right)}{k_2{}^2c^2}+\frac{4\omega_1{}^2}{\epsilon_0\,k_2{}^2c^2}\phi(E_1E_1^*)=0$$

$$(15)\quad -\frac{\partial A_2{}^2}{\partial z}\frac{\partial S_2}{\partial z}+\frac{\partial A_2^2}{\partial z}-\frac{\partial A_2^2}{\partial r}\frac{\partial S_2}{\partial r}-A_2^2\left(\frac{\partial^2S_2}{\partial r^2}+\frac{1}{r}\frac{\partial S_2}{\partial r}\right)=0$$

In the paraxial ray approximation, $r^2 << r_0^2f_2^2$, where f_2 is the beam width parameter of second harmonic wave. We expand S_2 as $S_2 = f(z) + \beta_2r^2/2$, where β_2^{-1} represents the radius of curvatures of the wave front of the second harmonic wave. For an initially Gaussian beam, we may write

$$(16)\quad A_2^2=\frac{A_{20}^2}{f_2^2(z)}\exp\left[-\frac{2r^2}{r_0^2f_2^2}\right]$$

Substituting the values of S_2 and A_2^2 in Eqs. (14) and (15) and equating the coefficients of r^2 on both sides, we obtain

$$\beta_2 = \frac{1}{f_2}\frac{df_2}{dz} \tag{17}$$

$$\frac{d^2 f_2}{dz^2} = \frac{4}{k_2^2 r_0^4 f_2^3} - \frac{2\omega_1^2 A_{10}^2 f_2}{\varepsilon_0 c^2 k_2^2 r_0^2 f_1^4}\phi'\left(\frac{A_{10}^2}{2f_1^2}\right) \tag{18}$$

where $\phi'(A_{10}^2/2f_1^2) = (\epsilon_S \epsilon_2/\epsilon_0)\exp(-\epsilon_2 A_{10}^2/2\epsilon_0 f_1^2)$.

The particular integral of Eq. (12) may be expressed as,

$$E_{22} = A_2^{'}\exp[-i\{2\omega_1 t - (2k_1 + k_0)z\}]$$

where

$$A_2^{'} = A_{20}^{'}(z)\psi_2, \psi_2 = \exp[-r^2/r_0^2 f_1^2]\exp[-2ik_1 S_1].$$

Substitute E_{22} in Eq. (12), we obtain

$$\begin{aligned} &4ik_1\psi_2\frac{\partial A_{20}^{'}}{\partial z} \\ &+\left[\frac{4\omega_1^2 - 5\omega_p^2}{c^2} + \frac{4\omega_1^2}{c^2}\phi(E_1E_1^*) - (2k_1+k_0)^2\right] \\ &\times A_{20}^{'}\psi_2 + A_{20}^{'}\frac{\partial^2\psi_2}{\partial r^2} + A_{20}^{'}\frac{1}{r}\frac{\partial\psi_2}{\partial r} \\ &= -\frac{\omega_p^2 e^2 B_W A_{10}^2}{2c^3\omega_1 m_0^2\gamma(\omega_1+iv)f_1^2}\left[\frac{3k_1}{4\omega_1} + \frac{k_1+k_0}{\omega_1+iv}\right]\exp\left[\frac{-r^2}{r_0^2 f_1^2}\right] \end{aligned} \tag{19}$$

Multiplying the above equation by $\psi_2^* r dr$ and integrating with respect to r, we get

$$\begin{aligned} &\frac{\partial A_{20}^{''}}{\partial\xi} + \left[\begin{array}{l} \dfrac{2\omega_1^2 r_0^2}{ic^2} - \dfrac{5\omega_1^2 r_0^2}{2ic^2}\dfrac{\omega_{p_0}^2}{\gamma\omega_1^2}\tan\left(\dfrac{\xi}{d}\right) + \dfrac{2\omega_1^2 r_0^2}{ic^2}\dfrac{\varepsilon_s}{\varepsilon_0} \\ -\dfrac{2\omega_1^2 r_0^2}{ic^2}\dfrac{\varepsilon_s}{\varepsilon_0}\exp\left(-\dfrac{b}{2f_1^2}\right) \\ -\dfrac{2\omega_1^2 r_0^2}{ic^2}\left(1 - \dfrac{1}{4}\dfrac{\omega_{p_0}^2}{\gamma\omega_1^2}\tan\left(\dfrac{\xi}{d}\right)\right) \\ +\dfrac{\omega_1^2 r_0^2}{ic^2}\dfrac{\varepsilon_s}{\varepsilon_0}\dfrac{\varepsilon_2 A_{10}^2}{\varepsilon_0}\dfrac{1}{4f^2} \\ \cdot\exp\left(-\dfrac{b}{2f_1^2}\right) - \dfrac{1}{2if_1^2} - \dfrac{1}{2i}\left(\dfrac{\partial f_1}{\partial\xi}\right)^2 \end{array}\right] A_{20}^{''} \\ &= -\frac{eA_{10}}{8f_1^2\gamma m_0\omega_1 c}\frac{\omega_1^2 r_0^2}{ic^2}\frac{\omega_c}{\omega_1}\frac{\omega_{p_0}^2}{\omega_1^2}\tan\left(\frac{\xi}{d}\right) \\ &\cdot\left[8\left(1 - \frac{\omega_{p_0}^2}{4\gamma\omega_1^2}\tan\left(\frac{\xi}{d}\right)\right)^{1/2} - \left(1 - \frac{\omega_{p_0}^2}{\gamma\omega_1^2}\tan\left(\frac{\xi}{d}\right)\right)^{1/2}\right] \end{aligned} \tag{20}$$

where $A_{20}^{''} = A_{20}^{'}/A_{10}$ is the normalized second harmonic amplitude.

Equation (20) describes the variation of normalized amplitude of the second harmonic wave $A_{20}^{''}$ with normalized propagation distance ξ.

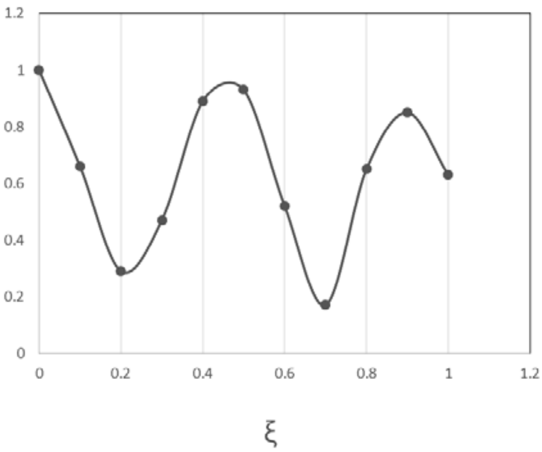

Fig. 1. Variation of beam width parameter of the fundamental laser beam with normalized propagation distance for, $\varepsilon_2 A_{10}^2/\varepsilon_0 = 5$, $\omega_{p0}/\omega_1 = 0.8$, and $a_{10} = 0.2$.

Result and discussion

We have solved Eqs. (11) and (20) numerically for beam width parameter and normalized second harmonic amplitude by applying the boundary conditions, corresponding to an initial plane wave front, at $\xi = 0$, $f_1 = 1$, $\partial f_1/\partial\xi = 0$, and at $\xi = 0$, $A_{20}^{''} = 0$. Normalized set of parameters of laser and plasma are used as; $\omega_c = eB_W/m_0 c$, $A_{20}^{''} = A_{20}^{'}/A_{10}$, $a_{10} = eA_{10}/m_0\omega_1 c$. For a typical case, plasma irradiated by a 1.06 μm Nd:YAG laser (intensity $I_0 \approx 5 \times 10^{17}$ W/cm^2), Wiggler magnetic field $B_W = 100$ kG, the Wiggler period turns out to be ≈ 0.2 cm, which is technically feasible even mega-gauss magnetic field can be generated [9]. Self-focusing occurs only when incident laser power exceeding the critical power. For high intensity laser, the critical power $P_{cr}(W) = 2.16 \times 10^{13}/n_0$ [cm^{-3}] mainly depends on electron density. Figure 1 shows the variation of beam width parameter of the fundamental laser beam with normalized propagation distance for, $\varepsilon_2 A_{10}^2/\varepsilon_0 = 5$, $\omega_{p0}/\omega_1 = 0.8$ and $a_{10} = 0.2$. It can be seen from Fig. 1 that strong self-focusing occurs at $\xi = 0.7$, $f_1 = 0.17$, due to the dominance of nonlinear term in Eq. (11). Figure 2 shows the variation of normalized second harmonic amplitude with the propagation distance for different values of $\omega_{p0}/\omega_1 = 0.2, 0.4, 0.6, 0.8$. The other parameters are the same as taken in Fig. 1. A sharp increase in the normalized second harmonic amplitude is seen for $\omega_{p0}/\omega_1 = 0.8$ at $\xi = 0.7$. Therefore, efficiency of second harmonic generation increases greatly with the increase in plasma frequency in the focal region of fundamental laser beam.

Figure 3 shows the variation of normalized second harmonic amplitude with the propagation distance for different values of $\omega_c/\omega_1 = 0.2, 0.4, 0.6, 0.8$, the other parameters are the same as taken in Fig. 1. One can clearly see that the normalized second harmonic amplitude increases with the increase in the Wiggler magnetic field strength in the focal region. Therefore, efficiency of second harmonic generation increases greatly with the increase in Wiggler magnetic field on account of the self-focusing of fundamental laser beam. Efficiency of second harmonic generation is affected by the strength of the Wiggler magnetic field. The dynamics of oscillating electrons is changed due to the Lorentz force which modifies the plasma wave which affects the second harmonic significantly. The second harmonic amplitude increases with the strength of the Wiggler magnetic field. Figure 4 shows the variation of normalized second harmonic amplitude with the propagation distance for different values of normalized fundamental intensity parameters, a_{10} = 0.2, 0.4, 0.6, 0.8, 1. The other parameters are $\varepsilon_2 A_{10}^2/\varepsilon_0 = 5$, $\omega_{p0}/\omega_1 = 0.8$ and $\omega_c/\omega_1 = 0.8$. It is clear from Fig. 4 that as we increase the intensity of the fundamental laser beam, the efficiency of second harmonic increases in the focal region. Figure 5 shows the variation of maximum normalized second harmonic amplitude with normalized intensity of fundamental laser beam a_{10} at $\xi = 0.7$ for $\varepsilon_2 A_{10}^2/\varepsilon_0 = 5$, $\omega_{p0}/\omega_1 = 0.8$ and $\omega_c/\omega_1 = 0.8$. This shows the linear variation of the normalized second harmonic amplitude with normalized fundamental intensity. As the electron plasma density is an increasing function of distance of propagation of laser, the diffraction length reduces as beam propagates deeper into the plasma. Hence the relativistic self-focusing of fundamental laser beam becomes stronger. Significant enhancement in the second harmonic yield is seen with increase in the laser beam intensity as well as with increase in plasma density. Thus, laser power and plasma density parameters are crucial to harmonic generation [25]. We observe the enhancement in the second harmonic on account of the relativistic self-focusing of laser in plasma under plasma density ramp in the presence of Wiggler magnetic field. Therefore, Wiggler magnetic field and relativistic self-focusing combindly play an important role in the enhancement of the intensity of the second harmonic wave. As the Wiggler magnetic field increases, the second harmonic intensity also increases.

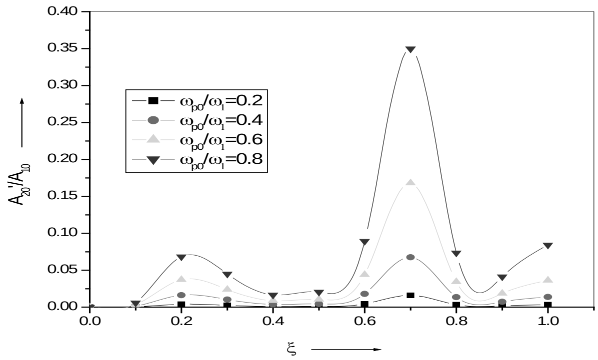

Fig. 2. Variation of normalized second harmonic amplitude with the normalized propagation distance for $\varepsilon_2 A_{10}^2/\varepsilon_0 = 5$, $\omega_c/\omega_1 = 0.8$, and $a_{10} = 0.2$.

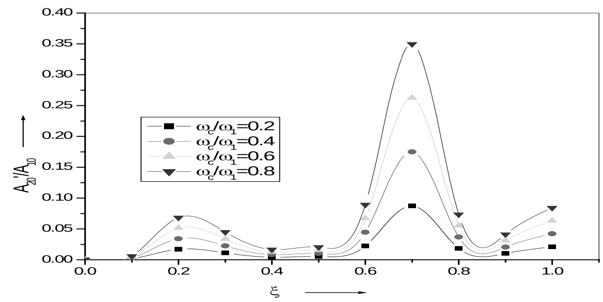

Fig. 3. Variation of normalized second harmonic amplitude with the normalized propagation distance for $\varepsilon_2 A_{10}^2/\varepsilon_0 = 5$, $\omega_{p0}/\omega_1 = 0.8$, and $a_{10} = 0.2$.

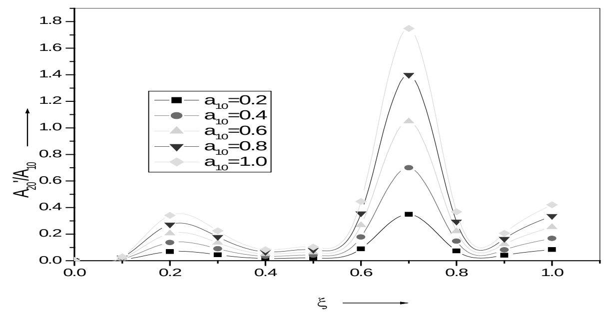

Fig. 4. Variation of normalized second harmonic amplitude with the propagation distance for $\varepsilon_2 A_{10}^2/\varepsilon_0 = 5$, $\omega_{p0}/\omega_1 = 0.8$, and $\omega_c/\omega_1 = 0.8$.

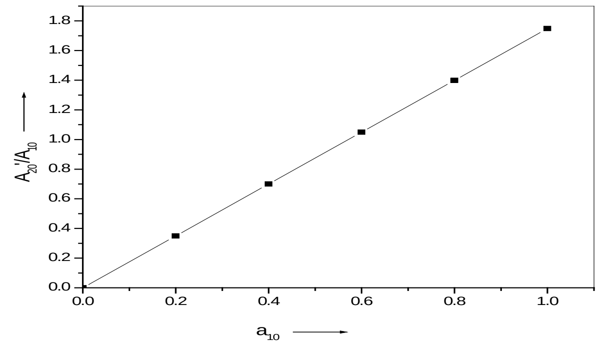

Fig. 5. Variation of normalized second harmonic amplitude with normalized intensity of fundamental laser beam a_{10} for $\varepsilon_2 A_{10}^2/\varepsilon_0 = 5$, $\omega_{p0}/\omega_1 = 0.8$, and $\omega_c/\omega_1 = 0.8$.

Conclusion

A slowly varying plasma density ramp plays an important role in the laser–plasma interaction. The density ramp may be important to make the self--focusing of short laser pulses stronger [26–29] if the laser and plasma parameters are chosen in an appropriate way. In the present work we have seen the strong relativistic self-focusing of laser beam based on plasma density transition which leads to enhance the second harmonic generation in the plasma under the influence of Wiggler magnetic field. With the increase of Wiggler magnetic field the intensity of second harmonic generation increases. It is seen that the normalized second harmonic amplitude increases linearly with normalized fundamental intensity a_{10}. Kuo *et al*. [22] have studied the enhancement of relativistic harmonic generation by an optically preformed periodic plasma waveguide. But in the present study we observe efficient second harmonic generation on account of strong relativistic self-focusing of the fundamental laser beam in plasma under plasma density ramp. The present analysis is useful in making the second harmonic efficient which may be effective in understanding the physics of laser–plasma interaction. Efficient second harmonic signals are capable of reading four times smaller area of DVD's as compare to the fundamental signals. Second harmonic polarization anisotropy can be used to find the orientation of proteins in tissues as they have well-defined polarizations.

References

1. Sharma, J. K., & Parashar, J. (2003). Parametric instability of a lower hybrid wave in a dusty plasma. *Indian J. Pure Appl. Phys.*, *41*, 290–294.
2. Sharma, J. K., Parashar, J., & Mehta, A. S. (2003). Relativistic stimulated Raman scattering in a plasma channel. *Indian J. Pure Appl. Phys.*, *41*, 73–76.
3. Parasher, J., & Pandey, H. D. (1992). Second--harmonic generation of laser radiation in a plasma with a density ripple. *IEEE Trans. Plasma Sci.*, *20*, 996–999. DOI: 10.1109/27.199564.
4. Parashar, J., & Sharma, A. K. (1998). Second harmonic generation by an obliquely incident laser on a vacuum plasma interface. *Europhys. Lett.*, *41*, 389. DOI: 10.1209/epl/i1998-00162-1.
5. Pramanik, T. K., & Bhattacharya, D. P. (1990). Harmonic generation in semiconductors in the presence of deep repulsive traps. *Solid State Commun.*, *74*, 539–542. DOI: 10.1016/0038-1098(90)90342-9.
6. Malka, V., Modena, A., Najmudin, Z., Dangor, A. E., Clayton, C. E., Marsh, K. A., Joshi, C., Danson, C., Neely, D., & Walsh. F. N. (1997). Second harmonic generation and its interaction with relativistic plasma waves driven by forward Raman instability in underdense plasmas. *Plasma Phys.*, *4*, 1127–1131. DOI: 10.1063/1.872201.
7. Esarey, E., Ting, A., Sprangle, P., Umstadter, D., & Liu, X. (1993). Nonlinear analysis of relativistic harmonic generation by intense lasers in plasmas. *IEEE Trans. Plasma Sci.*, *21*, 95–104. DOI: 10.1109/27.221107.
8. Kant, N., Gupta, D. N., & Suk, H. (2011). Generation of second-harmonic radiations of a self-focusing laser from a plasma with density-transition. *Phys. Lett. A*, *375*, 35. DOI: 10.1016/j.physleta.2011.06.062.
9. Tatarakis, M., Watts, I., Beg, F. N., Clark, E. L., Dangor, A. E., Gopal, A., Haines, M. G., Norreys, P. A., Wagner, U., Wei, M. S., Zepf, M., & Krushelnick, K. (2002). Laser technology-measuring huge magnetic fields. *Nature*, *415*, 280–280. DOI: 10.1038/415280a.
10. Kant, N., & Sharma, A. K. (2004). Resonant second--harmonic generation of a short pulse laser in a plasma channel. *J. Phys. D-Appl. Phys.*, *37*, 2395. DOI: 10.1088/0022-3727/37/17/009.
11. Petrov, E. Y., & Kudrin, A. V. (2010). Exact axisymmetric solutions of the Maxwell equations in a nonlinear nondispersive medium. *Phys. Rev. Lett.*, *104*, 190404-7. DOI: 10.1103/PhysRevLett.104.190404.
12. Kant, N., & Sharma, A. K. (2004). Effect of pulse slippage on resonant second harmonic generation of a short pulse laser in a plasma. *J. Phys. D-Appl. Phys.*, *37*, 998–1001. DOI: 10.1088/0022-3727/37/7/007.
13. Osman, F., Castillo, R., & Hora, H. (1999). Relativistic and ponderomotive self-focusing at laser–plasma interaction. *J. Plasma Phys.*, *61*, 263–273. DOI: 10.1017/S0022377898007417.
14. Hafizi, B., Ting, A., Sprangle, P., & Hubbard, R. F. (2000). Relativistic focusing and ponderomotive channeling of intense laser beams. *Phys. Rev. E*, *62*, 4120. DOI: 10.1103/PhysRevE.62.4120.
15. Hora, H., & Ghatak, A. K. (1985). New electrostatic resonance driven by laser radiation at perpendicular incidence in superdense plasmas. *Phys. Rev. A*, *31*, 3473. DOI: 10.1103/PhysRevA.31.3473.
16. Baton, S. D., Baldies, H. A., Jalinaud, T., & Labaune, C. (1993). Fine-scale spatial and temporal structures of second-harmonic emission from an underdense plasma. *Europhys. Lett.*, *23*, 191. DOI: 10.1209/0295-5075/23/3/006.
17. Schifano, E., Baton, S. D., Biancalana, V., Giulietti, A., Giulietti, D., Labaune, C., & Renard, N. (1994). Second harmonic emission from laser-preformed plasmas as a diagnostic for filamentation in various interaction conditions. *Laser Part. Beams*, *12*, 435. DOI: 10.1017/S0263034600008296.
18. Ganeev, R. A., Chakera, J. A., Raghuramaiah, M., Sharma, A. K., Naik, P. A., & Gupta, P. D. (2001). Experimental study of harmonic generation from solid surfaces irradiated by multipicosecond laser pulses. *Phys. Rev. E*, *63*, 026402. DOI: 10.1103/PhysRevE.63.026402.
19. Banerjee, S., Valenzuela, A. R., Shah, R. C., Maksimchuk, A., & Umstadter, D. (2002). High harmonic generation in relativistic laser–plasma interaction. *Phys. Plasmas*, *9*, 2393. DOI: 10.1063/1.1470167.
20. Lin, H., Chen, L., & Kieffer, J. C. (2002). Harmonic generation of ultraintense laser pulses in underdense plasma. *Phys. Rev. E*, *65*, 036414. DOI: 10.1103/PhysRevE.65.036414.
21. Mori, M., Takahashi, E., & Kondo, K. (2002). Image of second harmonic emission generated from ponderomotively excited plasma density gradient. *Phys. Plasmas*, *9*, 2812. DOI: 10.1063/1.1481506.
22. Kuo, C. C., Pai, C. H., Lin, M. W., Lee, K. H., Lin, J. Y., Wang, J., & Chen, S. Y. (2007). Enhancement of relativistic harmonic generation by an optically preformed periodic plasma waveguide. *Phys. Rev. Lett.*, *98*, 033901. DOI: 10.1103/PhysRevLett.98.033901.
23. Kant, N., Sarlach, S., & Singh, H. (2011). Ponderomotive self-focusing of a short laser pulse under a plasma density ramp. *Nukleonika*, *56*(2), 149–153.
24. Gupta, D. N., Hur, M. S., & Suk, H. (2006). Energy exchange during stimulated Raman scattering of a relativistic laser in plasma. *J. Appl. Phys.*, *100*, 103101-5. DOI: 10.1063/1.2384808.
25. Singh, A., & Walia, K. (2011). Self-focusing of Gaussian laser beam through collisionless plasmas and its effect on second harmonic generation. *J. Fusion Energy*, *30*, 555–560. DOI: 10.1007/s10894-011-9426-z.
26. Kant, N., Wani, M. A., & Kumar, A. (2012). Self--focusing of Hermite-Gaussian laser beams in plasma under plasma density ramp. *Opt. Commun.*, *285*, 4483–4487. DOI: 10.1063/1.4870080.
27. Nanda, V., Kant, N., & Wani, M. A. (2013). Self--focusing of a Hermite-cosh Gaussian laser beam in a magnetoplasma with ramp density profile. *Phys. Plasmas*, *20*, 113109-7. DOI: 10.1063/1.4870080.
28. Nanda, V., & Kant, N. (2014). Enhanced relativistic self-focusing of Hermite-Cosh-Gaussian (HChG) laser beam in plasma under density transition. *Phys. Plasmas*, *21*, 042101-6. DOI: 10.1063/1.4870080.
29. Nanda, V., & Kant, N. (2014). Strong self-focusing of a cosh-Gaussian Laser Beam in collisionless magnetoplasma under plasma density ramp. *Phys. Plasmas*, *21*, 072111-8. DOI: 10.1063/1.4889862.